Two-photon absorption and blue-light-induced red absorption in $LiTaO_3$ waveguides

Andy Carson and Matthew E. Anderson

Department of Physics, San Diego State University, San Diego, California 92182

Received September 15, 2005; revised December 15, 2005; accepted January 12, 2006; posted February 6, 2006 (Doc. ID 64806)

Two-photon absorption and blue-light-induced red absorption (BLIRA) is demonstrated in lithium tantalate ($LiTaO_3$) waveguides with ultrashort laser pulses. The blue transmission is modeled for hyperbolic-secant-squared pulses of blue light and is shown to be heavily attenuated by two-photon absorption. The blue light also generates traps for red light, which are absorbed through single-photon interactions. Over 50% red absorption is observed. The blue pulse energy dependence of BLIRA is shown to follow recent theoretical models that rely on two different physical mechanisms depending on the temporal overlap of the pump and probe pulses. The time dependence of BLIRA is explored experimentally and is shown to fit well to a stretched-exponential model. Finally, we investigate the effects of pulse shaping and find that, over our range of pulse durations, the amount of BLIRA is relatively insensitive to pulse shape.

OCIS codes: 190.7110, 230.7380, 320.7130.

1. INTRODUCTION

Femtosecond lasers have become the workhorse of the nonlinear optical community.[1] With their exceedingly high peak intensities, ultrashort laser pulses are responsible for illuminating various multiphoton processes, some by design, others by accident. Two such nonlinear processes that have recently garnered attention in the ultrafast regime are two-photon absorption[2,3] (TPA) and blue-light-induced red absorption[4] (BLIRA). TPA occurs in crystals when two photons have sufficient energy to span the bandgap of the material. Crystals that are essentially transparent to certain wavelengths can nonetheless absorb much of the incident light, provided that the beam is sufficiently intense. The higher the intensity and integrated optical path length, the greater the amount of TPA.

BLIRA, also known as blue-light-induced infrared absorption[5] or simply light-induced absorption,[6] is the absorption of a red probe beam in the presence of short-wavelength pump light. Although initially thought solely detrimental, it has recently been shown to be a valuable means for nonvolatile holographic storage.[7,8] The process arises owing to fundamental traps inherent in the bandgap. The traps can become populated via charge transfer from a strong blue pump beam and subsequently absorb red light. Since the charge transfer often occurs from the aforementioned TPA, this process is also nonlinear and therefore prevalent in short-pulse laser experiments.

Concurrent with the study of femtosecond nonlinear interactions has been the development of novel waveguide structures.[9,10] Specifically, quasi-phase-matched waveguides have been studied as a source of high-efficiency second-harmonic generators,[11] parametric amplifiers,[12] squeezers,[4,12–14] couplers,[15] and single-photon generators.[16] The small cross section and long interaction lengths make these devices ideal for nonlinear studies. When coupled with ultrashort laser pulses, they provide a unique and powerful tool to study high-intensity interactions with modest pulse energies.

In this article we present TPA and BLIRA in $LiTaO_3$ waveguides using femtosecond laser pulses. On the basis of new theoretical models by Beyer *et al.*,[17,18] we first remodel data that were not fully explained in this journal eight years ago[4] and then present new data consistent with these theoretical predictions.

2. THEORY

A. Two-Photon Absorption

TPA occurs in crystals for photons with energy greater than the half-bandgap. For $LiTaO_3$, the bandgap is 4.5–4.7 eV.[19] Blue photons at 400 nm correspond to 3.1 eV, which means that two blue photons have a combined energy well above the bandgap and will suffer from TPA. The formula for determining the transmitted blue energy for short hyperbolic-secant-squared pulses was presented in Ref. 4 and is presented here in slightly simpler form:

$$T = \frac{\exp(-\alpha_b L)}{\sqrt{u(u+1)}} \ln(\sqrt{u} + \sqrt{u+1}), \tag{1}$$

where

$$u = \frac{1.76 E_{\text{in}} \beta_b}{A_{\text{wg}} \tau \alpha_b} [1 - \exp(-\alpha_b L)], \tag{2}$$

the blue single-photon and TPA coefficients are given by α_b and β_b, respectively, L is the length of the waveguide, E_{in} is the input blue energy, A_{wg} is the cross-sectional area of the waveguide, and τ is the blue pulse duration. Note that in the limit that the TPA is negligible, by using low-energy pulses ($E_{\text{in}} \to 0$), long pulses ($\tau \to \infty$), or a low

TPA coefficient ($\beta_b \to 0$), the blue energy transmission returns to the single-photon absorption result [$T \to \exp(-\alpha_b L)$], as expected.

B. BLIRA: Direct Band–Band Transitions

$LiTaO_3$ is a relatively transparent crystal in the red and near-infrared spectral region. A red probe pulse will pass through the crystal unimpeded. However, should an intense blue pulse precede the red pulse, or indeed overlap with it in time, the red pulse will be strongly attenuated; the stronger the blue pulse, the greater the red attenuation. This BLIRA is strongest during temporal overlap with the blue pump pulse and gets progressively weaker as the red probe pulse arrives at subsequently later times. The dependence of BLIRA on the blue pump power was not well understood until recently, when Beyer *et al.*[17] presented a new physical model for its behavior.

In their model, the physical process is separated into two distinct components. Probe pulses that temporally overlap with the pump pulse can generate direct band–band transitions by absorbing a single blue photon and a single probe photon simultaneously, provided that their added energies are sufficient to span the gap. The amount of absorption is then governed by a product of the pump intensity, the probe intensity, and a new two-photon parameter β_r. In the moving frame, the red intensity is governed by

$$\frac{\partial I_r}{\partial x'} = -\beta_r I_r I_p. \tag{3}$$

With an input pump pulse and a probe pulse that are assumed to be Gaussian in both space and time, Beyer *et al.* show that this equation may be solved explicitly. In the case of a long crystal and short pulses, both broadening and dispersion need to be considered. Indeed, the pump will dramatically change its shape as it progresses through the crystal and suffers from TPA. Also, because the probe travels faster through the crystal than the pump, one would not expect the maximum BLIRA to occur when the pump and probe arrive at the crystal face simultaneously because the probe will quickly advance ahead of the pump and therefore not suffer any attenuation. With these effects, the amount of BLIRA corresponding to the immediate dip in transmission is given in Ref. 17 by the equation

$$A_r^{\mathrm{dip}} = 1 - T_r^{\mathrm{dip}}$$

$$= 1 - \frac{1}{\sqrt{\pi}} \int_{-\infty}^{\infty} \exp[-(s - \Delta t/t_p)^2] \times \int_0^1 \exp\left\{ -\frac{\beta_r}{\beta_b} \int_0^1 \frac{q_p f \mathrm{d}u}{q_p f u + \exp[(s - \delta_0 u)^2]} \right\} \mathrm{d}f \mathrm{d}s, \tag{4}$$

where Δt is the arrival time of the probe relative to the pump, t_p is the pump duration, q_p is a pumping parameter, and δ_0 is a phase-mismatch parameter. In our case, q_p has the value $q_p = (\eta \beta_b d E_{\mathrm{in}})/(\sqrt{\pi} t_p A_{\mathrm{wg}})$, where η is a waveguide coupling efficiency, d is the length of the waveguide, E_{in} is the input blue energy, and A_{wg} is the cross-sectional area of the waveguide. In Eq. (4), u, f, and s are dummy integration variables. This equation describes the attenuation of the probe versus blue pump energy. In the limit $E_{\mathrm{in}} = 0$ or ∞, the absorption becomes $A_r^{\mathrm{dip}} = 0$ or 1, respectively, as expected. The absorption shows a rapid rise with pump energy, followed by a strongly nonlinear saturation. We will show that this theory is adequate at modeling previously unexplained results from Refs. 4 and 20.

C. BLIRA: Traps

A different physical mechanism is at work for probe pulses that arrive after the pump pulse. In this case, there is no longer a simultaneous band–band transition, but, instead, absorption of the probe beam takes place by photoexcited free carriers or shallow trap states or both. Indeed, Beyer *et al.*[17] argue that, for probe delays on picosecond time scales, the carriers that were excited by the pump are the dominant absorption process for the probe beam. For probe delays longer than a few picoseconds, shallow traps are the dominant absorber.

The equations that govern the production of free carriers are functionally equivalent to the equations that govern the production of traps, save for an extra factor that dictates the probability that a photoexcited electron will be caught in a trapping site. The production of traps were presented in Ref. 4 as

$$\frac{\mathrm{d}N_x}{\mathrm{d}t} = \frac{1}{\hbar\omega} \alpha_b I_b + \frac{\xi}{2\hbar\omega} \beta_b I_b^2, \tag{5}$$

where ξ is the trapping probability factor. For Gaussian pulses, and in the absence of single-photon blue absorption ($\alpha_b = 0$), this equation is functionally equivalent to Eq. (12) in Ref. 17; thus we may make use of their elegant analytic solution to arrive at the absorption of the red probe beam due to the traps

$$A_r^{\mathrm{trap}} = 1 - T_r^{\mathrm{trap}}$$

$$= 1 - \int_0^{\infty} \exp\left\{ -f - b q_p \left[\frac{\sqrt{\pi}}{2} \exp(-f) - \int_0^{\infty} \frac{\mathrm{d}s}{q_p + \exp[f + s^2]} \right] \right\} \mathrm{d}f, \tag{6}$$

where $b = (2\xi\sigma_X t_p)/(\hbar\omega\beta_b d)$ is a dimensionless parameter and σ_X is the red absorption cross section of the traps. In this model, the independent fitting parameters are therefore coupling parameter η and product $\xi\sigma_X$. Again, this equation has the proper limits. As $E_{\mathrm{in}} = 0$ or ∞, the absorption becomes $A_r^{\mathrm{trap}} = 0$ or 1, respectively. In this model the red absorption as a function of pump energy is nearly linear for moderate pump energies, and we will show that it adequately models our new experimental results.

D. BLIRA: Temporal Decay

Many studies of $LiNbO_3$ and $LiTaO_3$[6,21–23] have explained these induced absorption effects in terms of deep and shallow traps (relative to the conduction band). The deeper traps are presumably Fe^{2+} ions, either specifically

doped into the crystal or unintentionally present in the growth process, and the shallow traps are predominantly structural defects in the crystal whereby a Nb^{5+} or Ta^{5+} ion is located at a Li^{+} site. Electrons can populate the shallow sites by either direct transition from the deep traps or relaxation from the conduction band. When an electron gets trapped at this site, it forms a bound polaron, Nb_{Li}^{4+} or Ta_{Li}^{4+}, which is then capable of being reexcited by infrared wavelengths. At room temperature, these polarons eventually relax but can still be observed on millisecond time scales.

The temporal decay of these polaron states follows a stretched-exponential behavior, the Kohlrausch–Williams–Watts function.[24] The physical reasoning behind this functional form is presented by Wevering *et al.*,[6] where they detail the role of the deep and shallow traps. To summarize their description, the rate of polaron decay depends on the distance between polarons and deep traps. By assuming this decay rate is inversely proportional with physical distance between them and that their separation is statistically distributed throughout the crystal, Wevering *et al.* are able to recover a probability for the electron to still be trapped at the shallow level and show that this probability decays as a stretched exponential. The equation that describes the induced absorption coefficient α versus time is then

$$\alpha = \frac{1}{d} \ln\left[\frac{E_r^{\min}}{E_r(t)}\right] = \alpha_{\max} \exp[-(t/\tau)^{\beta}], \tag{7}$$

where $E_r^{\min}$ is the minimum recorded probe energy transmitted through the crystal (which occurs when the pump and probe overlap temporally), $E_r(t)$ is the probe energy at a delay time t, $\alpha_{\max}$ is the maximum absorption, τ is the polaron lifetime, and β is the stretching factor. The absorption is maximum at $t=0$ and returns to zero at $t=\infty$. We will use this model to explain our temporal data.

3. EXPERIMENT

A. Waveguides

The lithium tantalate waveguides used in this study were fabricated by Mool Gupta at Kodak (presently at Old Dominion). They are 7 mm long $LiTaO_3$ waveguides that employ quasi-phase matching (QPM). The waveguides were constructed by ion exchange, and QPM was fabricated by electric field poling. The waveguides are single mode at 840 nm and multimode in the blue. More detailed descriptions of these waveguides may be found in Refs. 4, 25, and 26.

B. Laser System

The pump pulse originates from a femtosecond Ti:sapphire laser. The laser system consists of a homebuilt Ti:sapphire oscillator generating pulses of 20–100 fs in duration. The oscillator pulses are amplified in an eight-pass chirped-pulse amplifier system (Del Mar Photonics Wedge-M) at a repetition rate of 250 Hz (picked to give 4 ms between pulses, suitable for temporal decay studies). Typical pulse widths after the amplifier are 50 fs, with energies of near 400 μJ and a center wavelength of 800 nm.

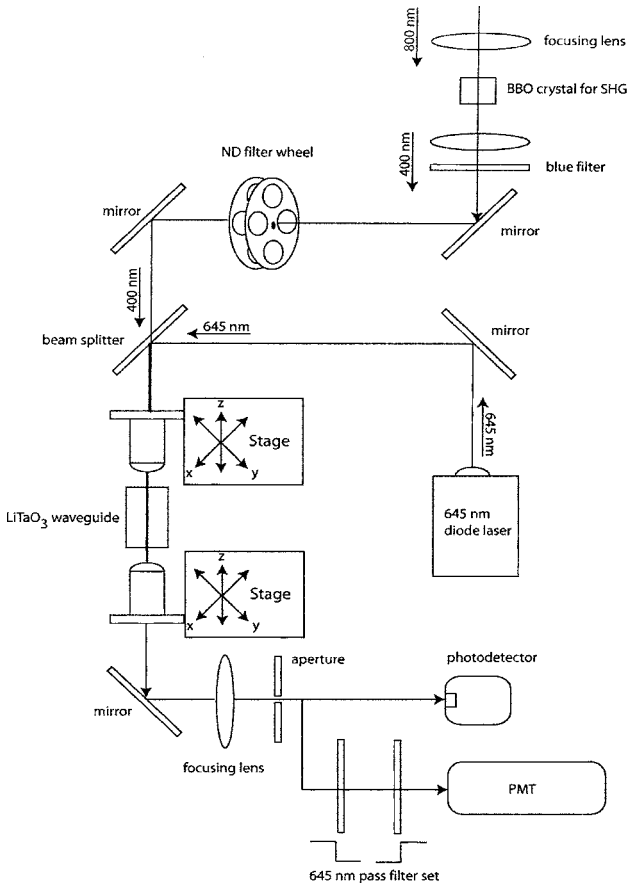

Fig. 1. Optical element layout for the TPA and BLIRA experiments. SHG, second-harmonic generation; NG; neutral-density; PMT, photomultiplier tube.

C. Two-Photon Absorption Apparatus

The experimental arrangement to measure TPA was fairly straightforward and is shown in Fig. 1. The laser pulses are loosely focused into a 0.5 mm type-II β-barium borate (BBO) crystal to generate second-harmonic light with an energy of approximately 10 μJ. Blue output from the BBO crystal was collimated by a lens (30 cm blue coated) and passed through a blue filter (Newport BG40) to remove unconverted red light from the amplifier. Further attenuation of this blue pulse was attained with a neutral-density (ND) filter wheel. The blue light was reflected off two steering mirrors before passing through a beam splitter (Newport 20RQ00UB.2), also shown in Fig. 1. Even though this beam splitter was not dichroic, reflective losses from the beam splitter were not a problem, since we had excess blue energy. The blue energy reflected from the beam splitter was monitored with a silicon photodiode as the ND filter wheel is rotated.

The waveguide coupling system consisted of two diode lenses (Thor Labs C240TM-A) placed at either end of the waveguide. The first diode lens was used to focus light into the waveguide, and the exit lens collected the transmitted light. Both lenses were mounted on x–y–z stages to aid in focusing and alignment. A standard inexpensive CCD camera (Supercircuits PC100XS) proved invaluable for looking at the transmitted light and identifying when coupling was optimum. When the focusing lens of the CCD camera was removed, the face of the waveguide

could be imaged directly on the CCD array. This gave a good picture of the face of the QPM crystal and the waveguides.

After blue pulses were coupled into the waveguide, both the input energy and the output energy were measured for a series of ND wheel settings. As the blue energy is increased, the blue transmitted energy increases in a nonlinear fashion. In fact, the blue transmission falls off quickly, making it difficult to adequately gauge the amount of blue light that is coupled into the waveguide. Our best coupling efficiency was approximately 20%, although individual runs varied greatly. Furthermore, since the blue pulses have traveled through several dispersive elements before reaching the waveguide, they are considerably lengthened in time. We estimate the duration of the pulses at the waveguide face to be nearly 1 ps.

D. BLIRA Apparatus

The experimental arrangement for BLIRA is also shown in Fig. 1. It simply requires the addition of a probe beam reflecting from the beam splitter and propagating collinearly with the blue pump pulse. The probe consists of a 645 nm pulsed diode laser (Thor Labs, Sanyo DL3147-021), with a pulse width of roughly 4 ns, and an arbitrary temporal delay set electronically by a digital delay box synched to the laser system (Stanford DG535). This system is versatile and allows the probe pulse to arrive before the pump, simultaneous with the pump, or at a delay of up to 4 ms following the pump (set by the 250 Hz repetition rate of the laser).

To get the initial alignment of the probe beam, we used a standard helium–neon (He–Ne) gas laser instead, since the average power was considerably greater. By carefully adjusting the steering mirrors and input x–y–z stage, it was possible to observe on the CCD camera when light was being coupled into a waveguide. Using the steering mirrors and horizontal translation of the crystal mount, it was possible to scan across the face of the crystal to select a waveguide that showed good coupling and mode quality. The mode was easily seen with the CCD camera. Once the diode lenses and waveguide were properly oriented and a reasonable amount of light from the He–Ne laser was being coupled into the waveguide, the He–Ne laser was replaced by the pulsed diode laser.

For performing the pump–probe experiments necessary for measuring the BLIRA effect, the blue and red light needed to be simultaneously coupled into the waveguide. Blue light that was transmitted through the beam splitter combined with the red light reflected off the front face of the beam splitter, as shown in Fig. 1. By observing the red and blue spots on a distant screen, we could adjust the steering mirrors so that the two beams were collinear entering the diode lens. One problem was that the diode focusing lens was not achromatic. Thus the red and blue light had slightly different focal points. This was offset somewhat by adjustment of the collimating lens after the second-harmonic-generation (SHG) crystal so that the blue light was slightly diverging when it entered the diode focusing lens before the waveguide. By careful adjustment, it was possible to have near-maximum blue coupling while still coupling in a significant amount of the red light. Because the value of interest was not the amount of red light but the relative strength of the red transmission with and without the blue pumping pulse present, maximizing the red coupling was not critical.

Light transmitted through the waveguide was collected and collimated with the second diode lens before passing through a pinhole aperture. The aperture served to cut down any light scattered around the waveguide crystal. After the pinhole the remaining light was focused and measured with either a standard photodetector (Thor Labs, DET210) or photomultiplier tube (PMT) (Hamamatsu 6199). The PMT allowed short and thus low-energy red probe pulses to be used. To reduce the background light level reaching the PMT, we used a set of two filters to create a bandpass notch at 645 nm, the wavelength of the diode laser. The first filter (Newport BG49) blocked residual infrared light from the amplified pulse and scattered fluorescence from the Ti:sapphire crystals. A second filter (Newport RG610) was used to block wavelengths shorter than 600 nm, effectively removing any remaining blue light from the BLIRA experiment and any scattered green light from the amplifier pump laser.

Measurements were sent via a Tektronix oscilloscope and general-purpose interface bus to a computer running LabView, in which the data were displayed and stored. LabView programs referred to as VIs were used to control most aspects of the experiment. Programs were written to control timing channels of the delay box and thus adjust the width of the red probe pulse and its temporal delay relative to the blue pumping pulse. Once working properly, the combination of laser optics, timing electronics, and controlling software allowed for the quick and relatively easy acquisition of data with little adjustment of the physical setup.

The laser system also contains a liquid-crystal pulse shaper (Cambridge Research SLM-256), capable of modulating both the amplitude and the phase of our pulses. This is done prior to amplification, and, since our amplification process does not reach saturation, good phase and amplitude shaping are maintained. The shaper was primarily used to add arbitrary phase profiles to the femtosecond pulse, to look for any dependence on the BLIRA level.

4. RESULTS AND DISCUSSION

A. Two-Photon Absorption Results

The experimental results for TPA are shown in Fig. 2. The data are shown with circles, and the theory is given by the solid curve. In all experiments, the fits were done using the Levenberg–Marquadt algorithm[27,28] (Igor Pro by WaveMetrics). The fit is excellent with a TPA coefficient given by $\sim 2\times 10^{-9}$ cm/W. Since our lowest-energy blue pulse was higher than previous studies, we scaled our coupling to match the results of Ref. 4. It is interesting to note that the amount of absorption is substantial. This is, of course, a testament to the high powers in ultrashort pulses but also results from the high intensity in the confined spatial modes of the waveguide. Short-pulse, high-intensity light, traveling through a long waveguide, is heavily absorbed through TPA, despite our use of relatively low-energy nanojoule pulses, compared with previous studies that used pulses in the 100 mJ range.[6]

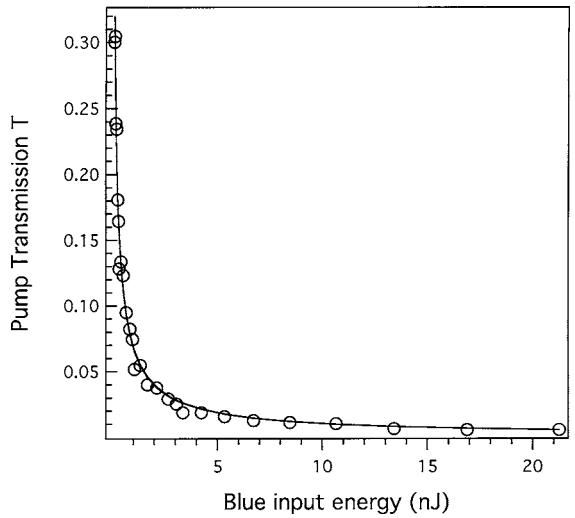

Fig. 2. TPA of the blue light. Blue transmission is plotted for increasing blue input pulse energy (circles) and compared with the TPA theory (solid curve) given by Eq. (1).

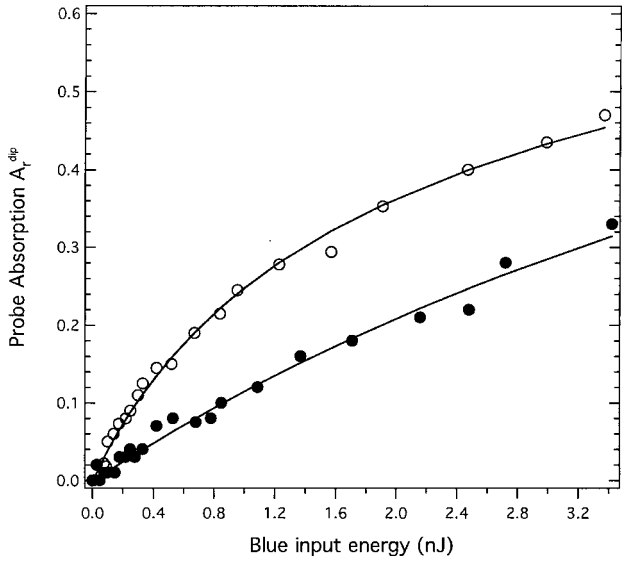

Fig. 3. BLIRA due to direct band–band transitions versus increasing blue pump energy. Markers show data for $t_p=1$ ps (open circles) and $t_p=4.4$ ps (filled circles). Solid curves, theoretical fits from Eq. (4).

B. BLIRA Results: Band–Band Transitions

BLIRA data previously reported in Refs. 4 and 20 are shown in Fig. 3, together with the theory from Eq. (4). There are two BLIRA experiments presented here. The first experiment uses a 1 ps pump and a 1 ps probe, shown with the open circles. The other uses a 4.4 ps pump and a 4.4 ps probe, shown with the filled circles. The theoretical fits from Eq. (4) are shown by the solid curves. In both of these experiments, the probe temporal delay was optically set to maximize the induced absorption. The values for the free parameters are as follows. For the $t_p=1$ ps data, we set the temporal delay to $\Delta t=1.3t_p$ (the maximum absorption) and found $\beta_r=0.79\beta_b$ and $\eta=0.18$. For the $t_p=4.4$ ps data, we set the temporal delay to $\Delta t=0.33t_p$ (the maximum absorption for this pump duration) and found $\beta_r=7.0\beta_b$ and $\eta=0.02$. Several comments about these parameters are warranted. The first is that the new theory of Beyer *et al.*[17] obviously does an excellent job at explaining the behavior of BLIRA versus pump energy, as shown by the high-quality fits. Second, the behavior of their theory is exactly as one would expect: short blue pulses generate more BLIRA than long blue pulses do. An obvious question arises, however. Why are the fit parameters different for the two experiments? For η, the likely difference is that the two experiments were vastly separated in time and optical layout. Thus, coupling efficiency could have changed dramatically (although it is a stretch to imagine a coupling coefficient of only 2%). For β_r, the likely culprit is carrier relaxation. As postulated in Ref. 17, there should be a change in absorption as hot carriers relax to the bottom of the conduction band, and this should happen on short time scales (<250 fs). Since both of the pulses (1 and 4.4 ps) are longer than this time, the absorption process is likely a combination of direct band–band transitions and trap-state absorption, and thus we would expect different parameters for their behavior. In fact, it is likely that the correct model for these pulse lengths would incorporate both absorption processes and require an extensive experimental search from ultrashort to several picosecond pulses, although that is beyond the scope of this article.

C. BLIRA Results: Traps

To illuminate the trap behavior, our experimental endeavor used a 1 ps pump pulse and a 4 ns probe pulse, and the results are shown in Fig. 4. Since a long probe pulse is used, the dynamics are substantially different from Eq. (4). Even though we temporally aligned the probe pulse to maximize BLIRA, the probe is roughly 4000 times longer than the pump pulse; thus we would expect extremely little contribution from direct band–band transitions. Instead, we use the model describing the absorption due to traps, given in Eq. (6). This is given by the solid curve in Fig. 4, with fitting parameters $\eta=0.05$ and product $\xi\sigma_x=2.95\times10^{-15}$ cm^2. This second parameter warrants discussion, as previous studies have resulted in cross sections in $LiNbO_3$ of the order of 10^{-17} cm^2 (Ref. 17). Thus, in our result, even if we let $\xi=1$, our traps are two orders of magnitude larger than bulk $LiNbO_3$. This could be an indication that in these

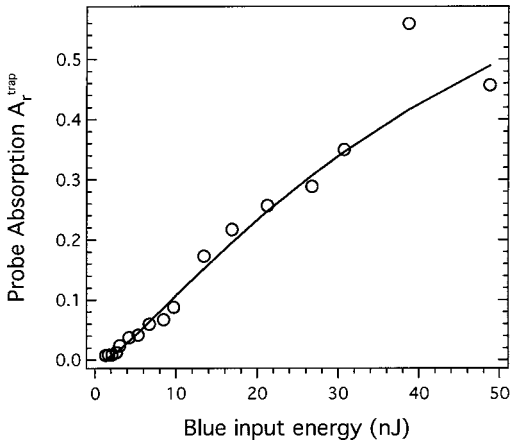

Fig. 4. BLIRA due to traps versus increasing blue pump energy. Circles, measured data; solid curve, a fit to Eq. (6).

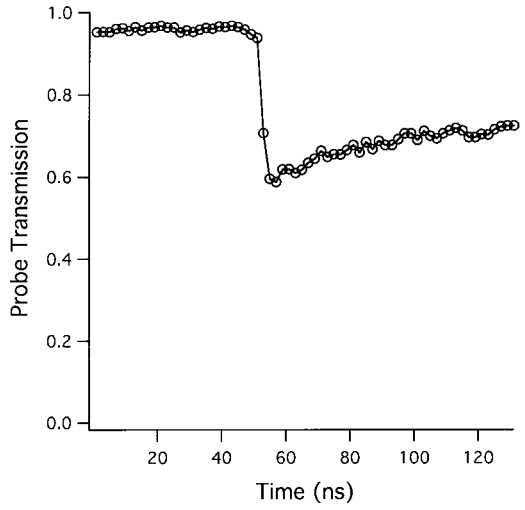

Fig. 5. Probe transmission versus temporal delay. The pump arrives at $t=56$ ns. The solid curve is simply a guide for the eye.

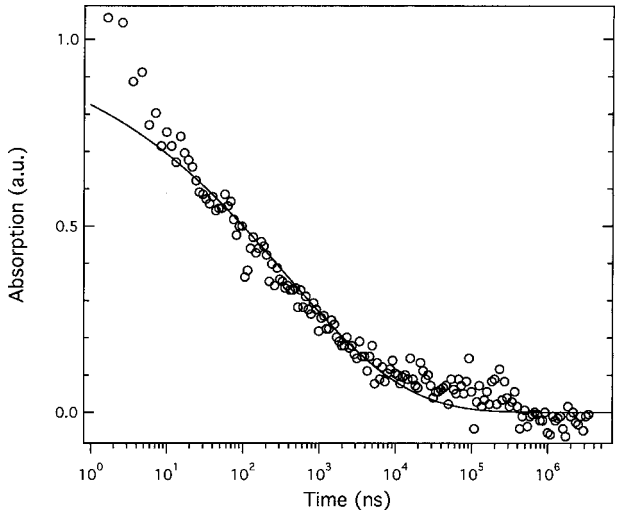

Fig. 6. Plot of the induced absorption change (relative to maximum) as a function of time. Circles, measured data; solid curve, a fit to Eq. (7).

QPM crystals, the ion-exchange process contributes to much larger trapping sites for red light. It is well known that, in $LiNbO_3$ crystals, nonstoichiometric defects play a particular role in interacting with trapped phonons to modify the electro-optic coefficient.[29,30] In the case of QPM waveguides,which possess higher structural disorder compared with single crystals, these effects may also play an important role. Systematically studying this behavior for waveguides with and without QPM would be beneficial. We should also mention that the weighting function for this fit excluded the last two points, as we discovered that the waveguide face was damaged at this blue energy level.

D. BLIRA Results: Temporal Decay

The transmission of the red probe pulse may also be monitored in time. This is shown in Fig. 5, where the red transmission is plotted versus temporal delay from the switched laser pulse. The strong dip in red transmission at $t=56$ ns is where the probe pulse aligns temporally with the blue pump pulse (the 56 ns delay is, in fact, how long it takes the femtosecond pulse to travel through the amplifier). The red transmission ultimately returns to unity in a few milliseconds. Since nanosecond probe pulses are used, the experiment is insensitive to the strong dip behavior observed by Beyer *et al.*[17,18] It is also interesting to note that the turn-on time is consistent with our probe duration. In fact, in all previous experiments, even with ultrashort probes, the turn-on time is essentially instantaneous; that is, it is governed by the probe duration.

We studied the temporal behavior of BLIRA's relaxation in greater detail, as shown in Fig. 6 where we have plotted absorption coefficient α versus probe delay time. The markers indicate our data, and the solid curve is a fit to Eq. (7), where we have normalized α_{max} to unity; the fitting parameters are $\tau=375$ ns and $\beta=0.28$. Note that the agreement is good except in the region $t<5$ ns. This is not unexpected, as this corresponds to our probe pulse duration. Note that this data are completely inexplicable by a monoexponential function. Indeed, the good agreement to the stretched exponential lends weight to the argument that polarons are the dominant trapping mechanism and that their statistical spatial distribution is indeed a primary factor in their decay behavior.[6] Our fit parameter $\beta=0.28$ is close to the range of values found by Wevering *et al.*,[6] but the parameter $\tau=375$ ns for our crystal was markedly different from their study, which revealed $\tau=10\,\mu$s with iron-doped $LiTaO_3$. Furthermore, in their study they demonstrate that the lifetime τ gets shorter with increasing iron concentration; thus it appears our waveguides are either heavily doped with iron (unintentionally) or that the QPM process leads to increased trap density. If the lifetime depends not only on the deep trap (iron) density but also on the shallow polaron concentration, this could neatly explain this phenomenon, since the QPM process is likely responsible for creating the structural defects behind polaron formation. Again, it would be useful to compare QPM and non-QPM waveguides to better observe this behavior.

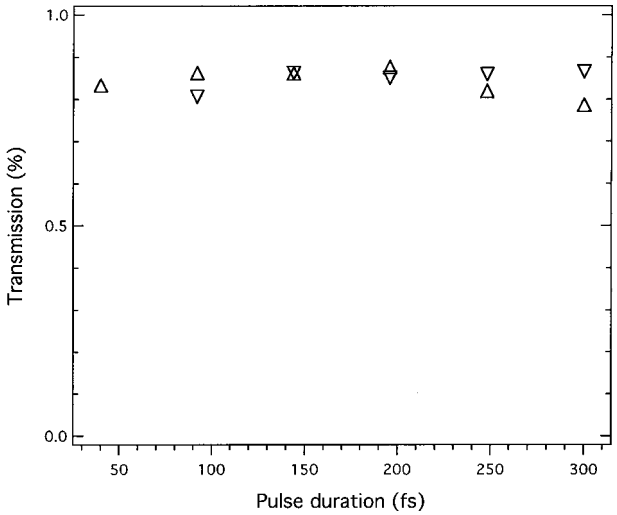

Fig. 7. Transmission of red pulses as a function of laser pulse duration. The markers indicate positive chirp (triangles) and negative chirp (inverse triangles).

E. BLIRA Results: Shaped Pulses

In an effort to determine if pulse duration or shape had any effect on the BLIRA signal, we also shaped the femtosecond pulses before the SHG crystal. To the limits of our pulse shaper, we were not able to uncover any dependence, including simple shapes such as spectral phase steps, changing bandwidths, and chirped pulses. An example of our results is shown in Fig. 7 where BLIRA was measured for varying amounts of chirp, both positive and negative. In all tests, we were careful to keep the total blue energy constant. As seen in Fig. 7, we were able to impart enough quadratic spectral phase to stretch our fundamental pulse by a factor of approximately 6, but no systematic effect on the BLIRA signal is seen. This is not unexpected when we consider several points. First, since the blue pulses are temporally dispersed by the optical elements, including the waveguide itself, they would likely not lengthen the pulse significantly even with highly chirped fundamental pulses. Thus, if a 50 fs fundamental pulse corresponds to a 1 ps blue pulse (after dispersion), a 300 fs chirped fundamental pulse would roughly correspond to a 1.3 ps blue pulse, a small fractional change in pulse length. Second, our waveguides are long, and, as seen in Fig. 2, the amount of blue TPA is significant. We suspect that a large amount of blue is absorbed whether the pulse is 1 or 1.3 ps. Since BLIRA is concerned with integrated trap density, which would be similar in the two cases, the amount of BLIRA should not change. Finally, our tests with spectral phase steps (not shown here) also indicated no change in BLIRA, testament that the TPA process is incoherent, as expected in broadband absorption processes. This is fundamentally different from TPA processes in narrowband transitions, for instance, in atoms.[31]

5. CONCLUSIONS

Studies of two-photon absorption and blue-light-induced red absorption in $LiTaO_3$ waveguides were presented. Ultrashort blue pulses are heavily attenuated in moderate-length waveguides, and the experimental evidence for TPA is overwhelmingly convincing. There seems to be little question that significant charge transfer is taking place owing to the presence of high-intensity light, especially when confined to a waveguide.

For BLIRA, the beautiful new theoretical work presented in Ref. 17 is compelling. With the inclusion of two physical mechanisms, direct band–band transitions and longer-lived trap states, it adequately models data that previously eluded proper explanation,[4,20] for pulses of 1 and 4.4 ps duration. Furthermore, the model works well for our new data using picosecond pump pulses and 4 ns probe pulses.

The relaxation of the polaron states follows the stretched-exponential model, presented in Ref. 6. It would be interesting to shore up the discrepancy for short delay times by using an ultrashort probe throughout, although it remains to be seen how one could delay this probe by a millisecond or more.

Our initial foray into pulse shaping indicated that TPA and BLIRA were not sensitive to pulse duration, phase, or chirp, at least with the system employed here. We suspect that a much shorter waveguide would be more sensitive to pulse duration, provided that there exists a means of delivering transform-limited pulses to the waveguide face, no small task. If one could, however, it would be beneficial to perform these experiments with pulses in the 10–50 fs range. Then, one could not only study the subtle effects of different pulse durations in more detail but also look for absorption changes due to hot-carrier relaxation, an area that has not yet been breached.

ACKNOWLEDGMENTS

The authors thank the generous assistance of Josh Thornes, Charlie Barnes, Mark Hatay, Mool Gupta, and Mike Raymer (in whose lab the work of Refs. 4 and 20 was performed). This work has been supported by the San Diego Foundation Blasker Grant, Research Corporation, and the Petroleum Research Fund.

Corresponding author M. E. Anderson can be reached by e-mail at matt@sciences.sdsu.edu.

REFERENCES

1. H. Kapteyn and M. Murnane, "Ultrashort light pulses: life in the fast lane," Phys. World **12**, 31–35 (1999).
2. E. W. Van Stryland, S. Guha, H. Vanherzeele, M. A. Woodall, M. J. Soileau, and B. S. Wherrett, "Verification of the scaling rule for two-photon absorption in semiconductors," Opt. Acta **33**, 381–386 (1986).
3. A. Villeneuve, C. C. Yang, G. I. Stegeman, C. N. Ironside, and G. Scelsi, "Nonlinear absorption in a GaAs waveguide just above half the band gap," IEEE J. Quantum Electron. **30**, 1172–1175 (1994).
4. M. E. Anderson, D. F. McAlister, M. G. Raymer, and M. C. Gupta, "Pulsed squeezed-light generation in $\chi^{(2)}$ nonlinear waveguides," J. Opt. Soc. Am. B **14**, 3180–3190 (1997).
5. E. S. Polzik and H. J. Kimble, "Frequency doubling and optical parametric oscillation with potassium niobate," Proc. SPIE **1561**, 143–146 (1991).
6. S. Wevering, J. Imbrock, and E. Kratzig, "Relaxation of light-induced absorption changes in photorefractive lithium tantalate crystals," J. Opt. Soc. Am. B **18**, 472–478 (2001).
7. A. Adibi, K. Buse, and D. Psaltis, "Two-center holographic recording," J. Opt. Soc. Am. B **18**, 584–601 (2001).
8. J. Imbrock, S. Wevering, K. Buse, and E. Kratzig, "Nonvolatile holographic storage in photorefractive lithium tantalate crystals with laser pulses," J. Opt. Soc. Am. B **16**, 1392–1397 (1999).
9. M. M. Fejer, "Nonlinear optical frequency conversion," Phys. Today **47**, 25–32 (1994).
10. M. M. Fejer, G. A. Magel, D. H. Jundt, and R. L. Byer, "Quasi-phase-matched second harmonic generation: tuning and tolerances," IEEE J. Quantum Electron. **28**, 2631–2654 (1992).
11. M. G. Roelofs, A. Suna, W. Bindloss, and J. D. Bierlein, "Characterization of optical waveguides in $KTiOPO_4$ by second harmonic spectroscopy," J. Appl. Phys. **76**, 4999–5006 (1994).
12. M. E. Anderson, M. Beck, M. G. Raymer, and J. D. Bierlein, "Quadrature squeezing with ultrashort pulses in nonlinear-optical waveguides," Opt. Lett. **20**, 620–622 (1995).
13. D. K. Serkland, M. M. Fejer, R. L. Byer, and Y. Yamamoto, "Squeezing in a quasi-phase-matched $LiNbO_3$ waveguide," Opt. Lett. **20**, 1649–1651 (1995).
14. D. K. Serkland, P. Kumar, M. A. Arbore, and M. M. Fejer, "Amplitude squeezing by means of quasi-phase-matched second-harmonic generation in a lithium niobate waveguide," Opt. Lett. **22**, 1497–1499 (1997).

15. R. Schiek, L. Friedrich, H. Fang, G. I. Stegeman, K. R. Parameswaran, M. H. Chou, and M. M. Fejer, "Nonlinear directional coupler in periodically poled lithium niobate," Opt. Lett. **24**, 1617–1619 (1999).
16. A. B. U'Ren, C. Silberhorn, K. Banaszek, and I. A. Walmsley, "Efficient conditional preparation of high-fidelity single photon states for fiber-optics quantum networks," Phys. Rev. Lett. **93**, 093601 (2004).
17. O. Beyer, D. Maxein, K. Buse, B. Sturman, H. T. Hsieh, and D. Psaltis, "Investigation of nonlinear absorption processes with femtosecond light pulses in lithium niobate crystals," Phys. Rev. E **71**, 056603 (2005).
18. O. Beyer, D. Maxein, K. Buse, B. Sturman, H. T. Hsieh, and D. Psaltis, "Femtosecond time-resolved absorption processes in lithium niobate crystals," Opt. Lett. **30**, 1366–1368 (2005).
19. C. Baumer, C. David, A. Tunyagi, K. Betzler, H. Hesse, E. Kratzig, and M. Wohlecke, "Composition dependence of the ultraviolet absorption edge in lithium tantalate," J. Appl. Phys. **93**, 3102–3104 (2003).
20. M. Anderson, "Squeezing in nonlinear optical waveguides," Ph.D. thesis (University of Oregon, 1998).
21. D. Berben, K. Buse, S. Wevering, P. Herth, M. Imlau, and T. Woike, "Lifetime of small polarons in iron-doped lithium–niobate crystals," J. Appl. Phys. **87**, 1034–1041 (2000).
22. F. Jermann and J. Otten, "Light-induced charge transport in $LiNbO_3$: Fe at high light intensities," J. Opt. Soc. Am. B **10**, 2085–2092 (1993).
23. P. Herth, D. Schaniel, T. Woike, T. Granzow, M. Imlau, and E. Kratzig, "Polarons generated by laser pulses in doped $LiNbO_3$," Phys. Rev. B **71**, 125128 (2005).
24. R. Kohlrausch, "Nachtrag über die Elastische Nachwirkung beim Cocon- und Glasfaden, und die Hygroskopische Eigenschaft des Ersteren," Pogg. Ann. Phys. **12**, 393–399 (1847).
25. C. Baron, H. Cheng, and M. C. Gupta, "Domain inversion in $LiTaO_3$ and $LiNbO_3$ by electric field application on chemically patterned crystals," Appl. Phys. Lett. **68**, 481–483 (1996).
26. V. Gopalan and M. C. Gupta, "Origin of internal field and visualization of 180° domains in congruent $LiTaO_3$ crystals," J. Appl. Phys. **80**, 6099–6106 (1996).
27. K. Levenberg, "A method for the solution of certain problems in least squares," Q. Appl. Math. **2**, 164–168 (1944).
28. D. Marquardt, "An algorithm for least-squares estimation of nonlinear parameters," SIAM J. Appl. Math. **11**, 431–441 (1963).
29. I. V. Kityk, M. Makowska-Janusik, M. D. Fontana, M. Aillerie, and F. Abdi, "Nonstoichiometric defects and optical properties in $LiNbO_3$," J. Phys. Chem. B **105**, 12242–12248 (2001).
30. I. V. Kityk, M. Makowska-Janusik, M. D. Fontana, M. Aillerie, and F. Abdi, "Band structure treatment of the influence of nonstoichiometric defects on optical properties in $LiNbO_3$," J. Appl. Phys. **90**, 5542–5549 (2001).
31. D. Meshulach and Y. Silberberg, "Coherent quantum control of two-photon transitions by a femtosecond laser pulse," Nature **396**, 239–241 (1998).